

Protein-tyrosine Phosphatase- α and Src Functionally Link Focal Adhesions to the Endoplasmic Reticulum to Mediate Interleukin-1-induced Ca^{2+} Signaling*

Received for publication, November 20, 2009, and in revised form, March 9, 2009. Published, JBC Papers in Press, June 3, 2009, DOI 10.1074/jbc.M808828200

Qin Wang[‡], Dhaarmini Rajshankar[‡], Donald R. Branch[§], Katherine A. Siminovitch^{¶1}, Maria Teresa Herrera Abreu[‡], Gregory P. Downey^{||**}, and Christopher A. McCulloch^{‡1,2}

From the [‡]Canadian Institutes of Health Research Group in Matrix Dynamics, Faculty of Dentistry, University of Toronto, Toronto, Ontario M5S 3E2, Canada, [§]Canadian Blood Services, Toronto, Ontario M5G 2M1, Canada, [¶]Samuel Lunenfeld Institute, Toronto, Ontario M5G 1X5, Canada, the ^{||}Division of Respiriology, Department of Medicine, University of Toronto, Toronto, Ontario M5G 1L7, Canada, and the ^{**}Division of Pulmonary and Critical Care Medicine, National Jewish Health, University of Colorado Denver Health Sciences Center, Denver, Colorado 80206

Calcium (Ca^{2+}) signaling by the pro-inflammatory cytokine interleukin-1 (IL-1) is dependent on focal adhesions, which contain diverse structural and signaling proteins including protein phosphatases. We examined here the role of protein-tyrosine phosphatase (PTP) α in regulating IL-1-induced Ca^{2+} signaling in fibroblasts. IL-1 promoted recruitment of PTP α to focal adhesions and endoplasmic reticulum (ER) fractions, as well as tyrosine phosphorylation of the ER Ca^{2+} release channel IP_3R . In response to IL-1, catalytically active PTP α was required for Ca^{2+} release from the ER, Src-dependent phosphorylation of $\text{IP}_3\text{R1}$ and accumulation of $\text{IP}_3\text{R1}$ in focal adhesions. In pull-down assays and immunoprecipitations PTP α was required for the association of PTP α with $\text{IP}_3\text{R1}$ and c-Src, and this association was increased by IL-1. Collectively, these data indicate that PTP α acts as an adaptor to mediate functional links between focal adhesions and the ER that enable IL-1-induced Ca^{2+} signaling.

The interleukin-1 (IL-1)³ family of pro-inflammatory cytokines mediates host responses to infection and injury. Impaired control of IL-1 signaling leads to chronic inflammation and destruction of extracellular matrices (1, 2), as seen in pathological conditions such as pulmonary fibrosis (3), rheumatoid arthritis (4, 5), and periodontitis (6). IL-1 elicits multiple signaling programs, some of which trigger Ca^{2+} release from the endoplasmic reticulum (ER) as well as expression of multiple cytokines and inflammatory factors including c-Fos and c-Jun

(7, 8), and matrix metalloproteinases (9, 10), which mediate extracellular matrix degradation via mitogen-activated protein kinase-regulated pathways (11).

In anchorage-dependent cells including fibroblasts and chondrocytes, focal adhesions (FAs) are required for IL-1-induced Ca^{2+} release from the ER and activation of ERK (12–14). FAs are actin-enriched adhesive domains composed of numerous (>50) scaffolding and signaling proteins (15–17). Many FA proteins are tyrosine-phosphorylated, including paxillin, focal adhesion kinase, and src family kinases, all of which are crucial for the assembly and disassembly of FAs (18–21). Protein-tyrosine phosphorylation plays a central role in regulating many cellular processes including adhesion (22, 23), motility (24), survival (25), and signal transduction (26–29). Phosphorylation of proteins by kinases is balanced by protein-tyrosine phosphatases (PTP), which can enhance or attenuate downstream signaling by dephosphorylation of tyrosine residues (30–32).

PTPs can be divided into two main categories: receptor-like and intracellular PTPs (33). Two receptor-like PTPs have been localized to FA (leukocyte common antigen-related molecule and PTP α). Leukocyte common antigen-related molecule can dephosphorylate and mediate degradation of p130^{cas}, which ultimately leads to cell death (34, 35). PTP α contains a heavily glycosylated extracellular domain, a transmembrane domain, and two intracellular phosphatase domains (33, 36). The amino-terminal domain predominantly mediates catalytic activity, whereas the carboxyl-terminal domain serves a regulatory function (37, 38). PTP α is enriched in FA (23) and is instrumental in regulating FA dynamics (39) via activation of c-Src/Fyn kinases by dephosphorylating the inhibitory carboxyl tyrosine residue, namely Tyr⁵²⁹ (22, 40–42) and facilitation of integrin-dependent assembly of Src-FAK and Fyn-FAK complexes that regulate cell motility (43). Although PTP α has been implicated in formation and remodeling of FAs (44, 45), the role of PTP α in FA-dependent signaling is not defined.

Ca^{2+} release from the ER is a critical step in integrin-dependent IL-1 signal transduction and is required for downstream activation of ERK (13, 46). The release of Ca^{2+} from the ER depends on the inositol 1,4,5-triphosphate receptor (IP_3R), which is an IP_3 -gated Ca^{2+} channel (47). All of the IP_3R subtypes (subtypes 1–3) have been localized to the ER, as well as

* This work was supported by a Canadian Institutes of Health Research Operating grant (to G. P. D. and C. A. M.).

¹ Supported by the Canada Research Chairs Program.

² To whom correspondence should be addressed: Rm. 244, Fitzgerald Bldg., University of Toronto, 150 College St., Toronto, ON M5S 3E2, Canada. Tel.: 416-978-1258; Fax: 416-978-5956; E-mail: christopher.mcculloch@utoronto.ca.

³ The abbreviations used are: IL, interleukin; PTP, protein-tyrosine phosphatase; ER, endoplasmic reticulum; ERK, extracellular signal-regulated kinase; FA, focal adhesion; IP_3 , inositol 1,4,5-triphosphate; IP_3R , IP_3 receptor; HA, hemagglutinin; GST, glutathione S-transferase; siRNA, short interfering RNA; PBS, phosphate-buffered saline; BSA, bovine serum albumin; PIPES, 1,4-piperazinediethanesulfonic acid; FN, fibronectin; PL, poly-L-lysine; GAPDH, glyceraldehyde-3-phosphate dehydrogenase; SFK, src family kinase.

PTP α and Focal Adhesions

other the plasma membrane and other endomembranes (48–50). Further, IP₃R may associate with FAs, enabling the anchorage of the ER to FAs (51, 52). However, the molecule(s) that provide the structural link for this association has not been defined.

FA-restricted, IL-1-triggered signal transduction in anchorage-dependent cells may rely on interacting proteins that are enriched in FAs and the ER (53). Here, we examined the possibility that PTP α associates with c-Src and IP₃R to functionally link FAs to the ER, thereby enabling IL-1 signal transduction.

EXPERIMENTAL PROCEDURES

Materials—Fibronectin, poly-L-lysine, doxycycline, radioimmune precipitation assay buffer, and mouse monoclonal antibodies to vinculin and β -actin were obtained from Sigma. Rabbit polyclonal antibodies to phospho-PTP α (Tyr⁷⁸⁹), as well as mouse monoclonal antibodies to phospho-Src (Tyr⁵²⁹ and Tyr⁴¹⁹) were from Cell Signaling (Beverly, MA). PTP α antibody directed against domain 2 was from Upstate Biotechnology Inc. (Lake Placid, NY). HA antibody was from Bethy Laboratories (Montgomery, TX). Mouse monoclonal anti-calnexin was obtained from BD Biosciences (Mississauga, Canada). Rabbit polyclonal anti-IP₃R1 was obtained from Affinity BioReagents (Golden, CO). Goat anti-integrin $\alpha 5\beta 1$ was purchased from Chemicon (Temecula, CA). FuGENE 6 transfection reagent and Fyn kinase were purchased from Invitrogen. Glutathione-Sepharose 4B, thrombin protease, GSTrap 4B, GSTrap FF, and HiTrap Benzamide FF were purchased from GE Healthcare. Recombinant human IL-1 β was obtained from R & D Systems (Minneapolis, MN). Fura-2/AM and mag-fura-2/AM were obtained from Molecular Probes, Inc. (Eugene, OR).

Cell Culture—Human gingival fibroblasts were grown in minimal essential medium containing 10% fetal bovine serum. Rat2 cells were maintained in Dulbecco's modified Eagle's medium containing 5% fetal bovine serum. Wild-type (PTP $\alpha^{+/+}$) and PTP α -null (PTP $\alpha^{-/-}$) fibroblasts were provided by Dr. Jan Sap (University of Copenhagen, Copenhagen, Denmark) (41). In some experiments, PTP $\alpha^{-/-}$ cells were transfected with wild-type PTP α and designated as PTP α Rescue. Genetically modified NIH3T3 fibroblasts that express HA-tagged wild-type PTP α (NIH3T3^{PTP α}) and C433S/C723S double mutant PTP α (NIH3T3^{C433S}) under control of a doxycycline sensitive repressor were obtained from David Shalloy (Department of Molecular Biology and Genetics, Cornell University, Ithaca, NY) and were generated as previously described (54). The latter cells were grown in Dulbecco's modified Eagle's medium containing 5% fetal bovine serum in the presence of 5 ng/ml doxycycline. Prior to experiments doxycycline was removed (14–16 h before) to allow expression of recombinant PTP α .

Plasmid Constructs and Transient Transfection—HA-tagged wild-type PTP α , PTP α lacking the D2 domain (PTP $\alpha^{\Delta D2}$) and PTP α lacking the D1 and D2 domains (PTP $\alpha^{\Delta D1/D2}$) were kindly provided by Dr. J. den Hertog (Hubrecht Laboratory, Netherlands Institute for Developmental Biology, Utrecht, The Netherlands). The cells were seeded in six-well plates at a density of 1×10^5 /well 24 h before transfection to yield a 30–40% confluent culture on the day of transfection. Transient trans-

fections were performed using FuGENE 6 transfection reagent (Roche Applied Science), according to the manufacturer's protocol. Briefly, the cells were incubated with DNA-FuGENE 6 reagent (1:3) complexes for 5–7 h. Within 48 h after transfection, the cells were subjected to further experiments.

Short Interfering RNA (siRNA)—Specific knockdown of PTP α expression was conducted with commercially available siRNA against PTP α (Qiagen). Human gingival fibroblasts were transfected with PTP α siRNA or GFP-siRNA (control) using X-tremeGENE siRNA transfection reagent (Roche Applied Science) according to the manufacturer's specifications. The cells were washed in PBS and lysed with SDS-lysis buffer. The lysates were collected, and measurement of the gene knockdown was performed 24–72 h after transfection by Western blotting.

Isolation of Focal Adhesions—The cells were grown to 80–90% confluence on 60-mm tissue culture dishes and were cooled to 4 °C prior to the addition of collagen or BSA-coated magnetite beads. Focal adhesion complexes were isolated from cells after specific incubation time periods as described (55). In brief, the cells were washed three times with ice-cold PBS to remove unbound beads and scraped into ice-cold cytoskeleton extraction buffer (0.5% Triton X-100, 50 mM NaCl, 300 mM sucrose, 3 mM MgCl₂, 20 μ g/ml aprotinin, 1 μ g/ml leupeptin, 1 μ g/ml pepstatin, 1 mM phenylmethylsulfonyl fluoride, 10 mM PIPES, pH 6.8). The cell-bead suspension was sonicated for 10 s (output setting 3, power 15% Branson), and the beads were isolated from the lysate using a magnetic separation stand. The remainder of the lysates was used to assess the non-focal adhesion fraction. The beads were resuspended in fresh ice-cold cytoskeleton extraction buffer, homogenized with a Dounce homogenizer (20 strokes), and reisolated magnetically. The beads were washed in CSKB, sedimented with a microcentrifuge, resuspended in Laemmli sample buffer, and placed in a boiling water bath for 3–5 min to allow the collagen-associated complexes to dissociate from the beads. The beads were sedimented, and lysates were collected for analysis.

Subcellular Fractionation—Subcellular fractionation was performed as previously described (56), and the cells were harvested, resuspended in an isotonic buffer (10 mM Tris, pH 7.6, 100 mM CaCl₂, 200 mM sucrose), and disrupted by Dounce homogenization followed by 20 strokes. The homogenate was spun at $800 \times g$ for 10 min, and the supernatant was recovered and further centrifuged for 10 min at $8,000 \times g$. The resulting supernatant was further spun for 1.5 h at $28,000 \times g$. The resulting pellet constituted the microsomal ER fraction. The specificity of the ER fraction was confirmed by immunoblotting with the ER-specific protein calnexin.

Immunoblotting—The protein concentrations of cell lysates were determined by Bradford assay (Bio-Rad). Equal amounts of protein were loaded onto SDS-polyacrylamide gels (10% acrylamide), resolved by electrophoresis, and transferred to nitrocellulose membranes. The membranes were incubated for 1 h at room temperature in Tris-buffered saline solution with 5% milk or 0.2% BSA to block nonspecific binding sites. The membranes were incubated with the primary antibodies overnight at 4 °C in Tris-buffered saline with 0.1% Tween 20. Horseradish peroxidase secondary antibodies were incubated for 1 h at room temperature in Tris-buffered saline with 0.1% Tween

20 and 5% milk or 0.2% BSA. Labeled proteins were visualized by chemiluminescence as per the manufacturer's instructions (Amersham Biosciences, Oakville, Canada).

Immunoprecipitation—The cells were lysed in radioimmune precipitation assay buffer (50 mM HEPES, pH 7.4, 1% deoxycholate, 1% Triton X-100, 0.1% SDS, 150 mM NaCl, 1 mM EDTA, 1 mM Na₃VO₄) containing 1 mM phenylmethylsulfonyl fluoride, 10 μ g/ml leupeptin, and 10 μ g/ml aprotinin. Equal amounts of protein from cleared extracts were subjected to standard immunoprecipitation or immunoblotting procedures.

GST Pulldown Experiments—GST-cPTP α (residues 167–793, full cytoplasmic domain), GST-PTP α D1 (residues 167–503, domain 1), and GST-PTP α D2 (residues 504–793, domain 2) were kindly provided by Dr. J. den Hertog (Hubrecht Laboratory, Netherlands Institute for Developmental Biology, Utrecht, The Netherlands). The cells were isolated by scraping and lysed for 10 min on ice in radioimmune precipitation assay buffer. The lysed cells were centrifuged at 900 \times *g* for 3 min to remove insoluble debris. The supernatants were removed and stored at -80°C until use. The cell lysates were precleared with 50 μ l of 50% slurry of glutathione-Sepharose 4B (1 \times PBS) and 25 μ g of GST for 2 h at 4 $^{\circ}\text{C}$. The Sepharose matrix was removed by centrifugation at 500 \times *g* for 5 min. The supernatants were subsequently incubated with 50 μ l of glutathione-Sepharose 4B, 5 mg of GST protein in PBS + 1% Triton X-100 with gentle agitation at room temperature for 30 min. The matrix was recovered by centrifugation at 500 \times *g* for 5 min. The glutathione-Sepharose 4B pellet was washed four times with 1 ml of PBS. GST was eluted from the glutathione-Sepharose 4B matrix by incubating twice with 50 μ l of elution buffer (10 mM reduced glutathione in 50 mM Tris-HCl, pH 8.0) for 10 min at room temperature and isolated by centrifugation at 500 \times *g* for 5 min and pooling the supernatants. The samples were boiled for 5 min and analyzed by immunoblotting.

In Vitro Phosphorylation—For *in vitro* phosphorylation using Fyn, immunoprecipitates bound to protein A-Sepharose beads were incubated for 10 min at room temperature in 20 μ l of kinase buffer (25 mM HEPES, pH 7.1, 10 mM MgCl₂, 5 mM MnCl₂, 0.5 mM EGTA, 1 mM Na₃VO₄, 1 mM dithiothreitol, 100 μ M MgATP) in the presence of 5 units of active Fyn. The reaction products were analyzed by immunoblotting using antibodies against phosphotyrosine.

Calcium Signals—For measurement of whole cell [Ca²⁺]_i, cells on coverslips were loaded with 3 μ M fura-2/AM for 20 min at 37 $^{\circ}\text{C}$. For estimating [Ca²⁺]_{ER}, the cells were incubated with mag-fura-2/AM (4 μ M) for 150 min at 37 $^{\circ}\text{C}$ in culture medium and measured by ratio fluorimetry as described (13). The nominally calcium-free buffer consisted of a bicarbonate-free medium containing 150 mM NaCl, 5 mM KCl, 10 mM D-glucose, 1 mM MgSO₄, 1 mM Na₂HPO₄, and 20 mM HEPES at pH 7.4 with an osmolarity of 291 mOsm. For experiments requiring external Ca²⁺, 2 mM CaCl₂ was added to the buffer; for experiments requiring chelation of external Ca²⁺, 1 mM EGTA was added. After incubation with fura-2/AM, inspection of cells by fluorescence microscopy demonstrated no vesicular compartmentalization of fura-2, suggesting that the dye loading method permitted measurement of cytosolic [Ca²⁺]_i. Visual inspection of mag-fura-2-loaded cells showed fluorescent labeling of intra-

cellular organelles. Whole cell [Ca²⁺]_i measurements and mag-fura-2 ratios were obtained with C-IMAGING SYSTEMS (Compix, Inc., Cranberry, PA) with excitation wavelengths of 340 and 380 nm and an emission wavelength of 520 nm. Changes in [Ca²⁺]_i were monitored by the ratio of fura-2 fluorescence at 340 and 380 nm.

Data Analysis—The means \pm S.E. were calculated for [Ca²⁺]_i measurements including base-line [Ca²⁺]_i, net change in [Ca²⁺]_i above base line, and the mag-fura-2 ratios. For continuous variables, the means \pm S.E. were computed, and when appropriate, comparisons between two groups were made with the unpaired Student's *t* test or with analysis of variance for multiple samples. Statistical significance was set at *p* < 0.05. For all of the experiments, *n* \geq 3 replicates were used.

RESULTS

PTP α Is Necessary for IL-1-induced Ca²⁺ Signaling—IL-1 triggers focal adhesion-dependent Ca²⁺ release from the ER (12, 57). Because PTP α is critical for regulating the formation and maturation of focal adhesions (23, 44), we determined whether PTP α regulates variations in the concentrations of cytoplasmic Ca²⁺ ([Ca²⁺]_i) and endoplasmic reticulum Ca²⁺ ([Ca²⁺]_{ER}) in response to IL-1. In PTP α wild-type primary murine fibroblasts (PTP α ^{+/+}), IL-1 treatment increased [Ca²⁺]_i and caused a transient release of Ca²⁺ from the ER (Fig. 1A). By contrast, the amplitude of IL-1-induced Ca²⁺ signals was reduced by >8-fold (*p* < 0.001) in PTP α -null primary mouse fibroblasts (PTP α ^{-/-}). Although IL-1-induced induced Ca²⁺ flux was fully restored by transfection with wild-type PTP α (PTP α ^{Rescue}; Fig. 1B), by comparison there was a >5-fold lower response (*p* < 0.001) in cells transfected with either PTP α ^{Δ D2} (PTP α lacking the catalytically active domain 2) or with PTP α ^{Δ D1/D2} (PTP α lacking both catalytic domains 1 and 2). Similarly cells expressing catalytically inert PTP α (C433S/C723S; designated NIH3T3^{CSS}; Fig. 1C) exhibited a >4-fold smaller [Ca²⁺]_i response and an 8-fold smaller [Ca²⁺]_{ER} response than cells expressing wild-type PTP α (designated NIH3T3^{PTP α}). Finally, in human gingival fibroblasts, knock-down of PTP α using siRNA resulted in a >6-fold (*p* < 0.001) lower amplitude of IL-1-induced [Ca²⁺]_i and [Ca²⁺]_{ER} responses (Fig. 1D). Taken together these data clearly indicate that intact catalytic activity of PTP α is essential for the IL-1-induced Ca²⁺ signaling.

Spatial Relationships between PTP α and FA- and ER-associated Proteins—The dependence of IL-1-induced Ca²⁺ signaling on PTP α motivated us to determine whether IL-1 affects the association of PTP α with focal adhesion- and ER-associated proteins. After IL-1 treatment, the relative abundance of PTP α and IP₃R1 (the ER calcium release channel isoform that is most abundant in fibroblasts (58)) was increased in focal adhesion preparations (which also contain substantial amounts of plasma membrane) and in ER fractions (Fig. 2A). By contrast, the relative abundance of the loading control proteins α 5 β 1 integrin (in focal adhesion fractions) and calnexin (in ER fractions) was unchanged by IL-1 treatment. We also found marked, IL-1-induced increases of vinculin in focal adhesion preparations, indicating that IL-1 enhanced the maturation of focal adhesions (44). Vinculin was almost undetectable in the ER fraction.

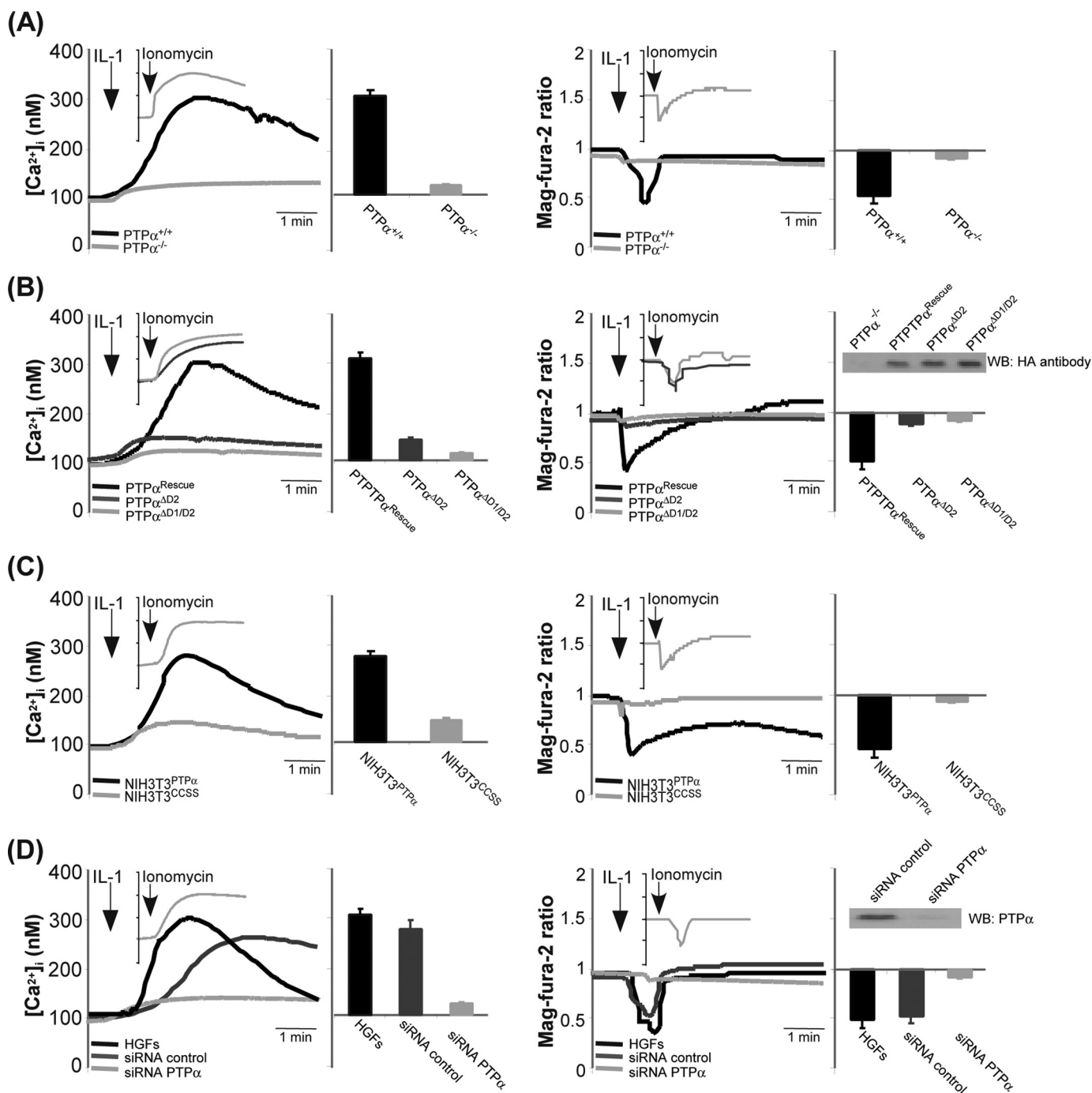


FIGURE 1. **PTP α is required for IL-1-induced Ca²⁺ release from the ER.** Intracellular calcium concentration ([Ca²⁺]_i) or mag-fura-2 ratios were measured in fura-2 or mag-fura-2-loaded cells after treatment with IL-1. *Insets*, ionomycin as positive control. *A*, response of PTP $\alpha^{+/+}$ and PTP $\alpha^{-/-}$ primary mouse fibroblasts cells. *B*, response of PTP α^{Rescue} , PTP $\alpha^{\Delta D2}$ and PTP $\alpha^{\Delta D1/\Delta D2}$ cells. *Inset*: Western blot for HA-tagged shows the presence of PTP α in cells transfected with mutant constructs. *C*, responses of NIH3T3^{PTP α} and NIH3T3^{CCSS} cells. *D*, responses of human gingival fibroblasts or human gingival fibroblasts transfected with irrelevant GFP-siRNA (siRNA control) and PTP α -siRNA (siRNA PTP α). *Inset*, Western blot for PTP α illustrates specific knockdown of PTP α in PTP α -siRNA treated cells.

We examined the localization of PTP α relative to focal adhesions and ER-associated proteins using total internal reflection fluorescence microscopy in cells plated on FN or BSA latex beads dispersed on poly-L-lysine substrates. Plating cells on poly-L-lysine coatings restricts focal adhesion formation to fibronectin bead sites in this system (58). Total internal reflection fluorescence microscopy analysis revealed that co-localization of IP₃R1 with PTP α occurred only after IL-1 treatment

and only around FN-coated (but not BSA-coated) beads (Fig. 2*B*).

The relative abundance of IP₃R1 and PTP α in whole cell lysates, focal adhesion preparations or ER fractions was examined by immunoblotting lysates prepared from PTP $\alpha^{-/-}$ cells or PTP $\alpha^{-/-}$ cells transfected with wild-type PTP α (PTP α^{Rescue}). IL-1 treatment enhanced accumulation of IP₃R1 in focal adhesions and ER fractions in PTP α^{Rescue}

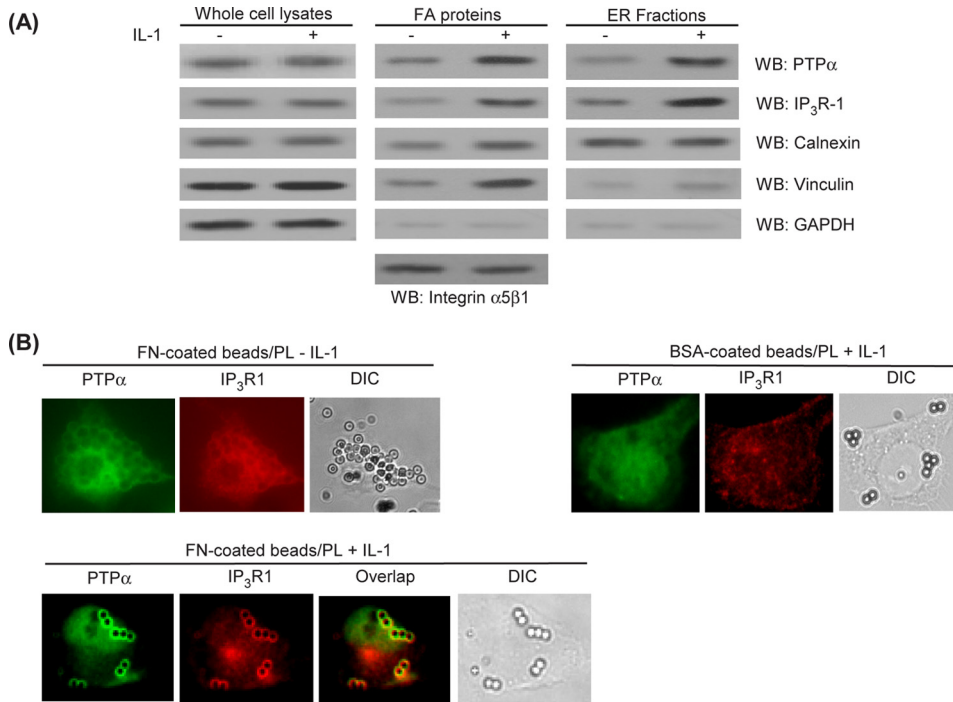


FIGURE 2. PTP α co-localizes with ER-associated proteins in focal adhesions. *A*, whole cell lysates, focal adhesion proteins, and ER fractions prepared from Rat2 cells previously treated with IL-1 (+) or vehicle (-). The lysates were immunoblotted for PTP α , IP₃R1, calnexin, vinculin, and GAPDH. *B*, Rat2 cells plated for 3 h on PL-coated glass coverslips that were preincubated with FN- or BSA-coated latex beads. In untreated cells or after stimulation with IL-1, the cells were co-immunostained for PTP α /IP₃R1 and viewed by fluorescence microscopy. *WB*, Western blotting.

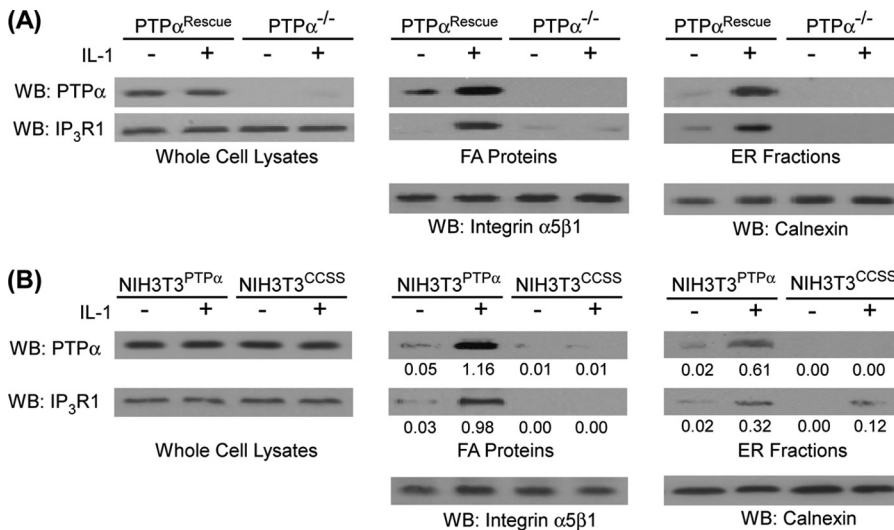


FIGURE 3. PTP α is required for IP₃R1 recruitment to focal adhesion and ER. Whole cell lysates, focal adhesion proteins, and ER fractions prepared from the following cells were immunoblotted for PTP α and IP₃R1 following induction with (+) or without (-) IL-1. *A*, PTP α ^{Rescue} cells or PTP α ^{-/-} cells transfected with wild-type PTP α (PTP α ^{Rescue}). *B*, NIH3T3^{PTP α} and NIH3T3^{CCSS} cells. The numbers beneath the blots in *B* represent the ratios of PTP α or IP₃R1 to the α 5 β 1 integrin or calnexin controls. *WB*, Western blotting.

cells but not in PTP α ^{-/-} cells (Fig. 3*A*). We next found that IL-1 promoted the recruitment of PTP α and IP₃R1 to focal adhesions and ER fractions in NIH3T3 cells expressing wild-type PTP α (NIH3T3^{PTP α}), but this effect was much smaller in NIH3T3^{CCSS} cells (Fig. 3*B*). Immunoblot analysis of PTP α immunoprecipitates from NIH3T3^{PTP α} cells showed that IP₃R1 co-precipitated with PTP α derived from whole cell lysates, focal adhesion preparations, and ER preparations,

and these associations were markedly increased after IL-1 treatment (Fig. 4*A*). By contrast, in NIH3T3^{CCSS} cells, almost no IP₃R1 co-precipitated with PTP α in cells expressing the catalytically inactive PTP α (Fig. 4*B*).

The associations of PTP α with IP₃R1 were examined with pull-down assays using purified GST-cPTP α (cytosolic domain), GST-PTP α D1 or GST-PTP α D2 fusion proteins incubated with cell lysates, focal adhesion proteins, or ER fractions prepared from PTP α ^{Rescue} cells. From immunoblots of IP₃R1, we found that the cytoplasmic and D1 domains of PTP α associated with IP₃R1 in the FA and ER fractions, more strongly than D2 domain (Fig. 5*A*). This association appeared to be direct because the purified, bacterially expressed GST fusion-cPTP α strongly bound to immunoprecipitated IP₃R1, whereas immunoprecipitated IP₃R1 showed no association with control GST beads (Fig. 5*B*).

IL-1 Regulates Tyrosine Phosphorylation of PTP α and Src to Mediate ER-Ca²⁺ Release—The optimum Ca²⁺ conductance of the IP₃R release channel in the ER requires the activity of SFK such as c-Src and Fyn (59, 60), which in turn are regulated by PTP α (30, 31, 61). Accordingly, when we examined the IL-1-induced Ca²⁺ release from the ER of PTP α ^{+/+} cells, the pronounced, short term release of Ca²⁺ was blocked in cells pretreated with the SFK inhibitors, SU6656, or PP2, but not in cells pretreated with the inactive structural analog PP3 (Fig. 6*A*).

The level of SFK activation can be estimated by the phosphotyrosine levels of inhibitory and stimulatory residues, Tyr⁵²⁹ and Tyr⁴¹⁹ in rodents, respectively (22, 40, 62).

First we examined the regulation of SFK activation using PTP α ^{+/+} cells plated either on fibronectin (FN) or on poly-L-lysine (PL), conditions that either facilitate or block FA formation, respectively (57). In otherwise unstimulated PTP α ^{+/+} cells, immunoblot analysis of whole cell lysates with antibody to phospho-Src (Tyr(P)⁵²⁹) revealed very low levels of phosphorylation of the inhibitory tyrosine in cells plated on FN (focal adhesions are present) compared with cells plated on PL (focal adhesions are absent; Fig. 6*B*). These data are con-

PTP α and Focal Adhesions

sistent with the observation that Src becomes activated via dephosphorylation of Tyr⁵²⁹ during adhesion and spreading on a fibronectin substrate, and this activation is dependent on and mediated by PTP α (24, 42). Further, in PTP $\alpha^{-/-}$ cells, there was abundant phosphorylation of the inhibitory residues (Tyr⁵²⁹) of Src that was unchanged after IL-1 treatment (Fig. 6B), consistent with previous reports (40, 63). In PTP $\alpha^{+/+}$ cells, there was a modest increase in phosphorylation of Tyr⁵²⁹ Src, after 15 min of IL-1 treatment (Fig. 6B). This IL-1-induced inhi-

bition of Src, however, was not evident at early time points, because the phosphorylation levels of inhibitory (Tyr⁵²⁹) and stimulatory (Tyr⁴¹⁹) residues were relatively unchanged (Fig. 6C).

We investigated whether the ability of PTP α to dephosphorylate Src diminishes over time after IL-1 treatment. The phosphotyrosine displacement model by Zheng *et al.* (54) proposes that phosphorylation of tyrosine 789 of PTP α selectively promotes its phosphatase activity toward Src by enabling association with the SH2 domain of Src. Accordingly, when whole cell lysates from PTP $\alpha^{+/+}$ cells were treated with IL-1 or vehicle and then immunoblotted for phospho-PTP α (Tyr(P)⁷⁸⁹), we observed that there was an initial IL-1-induced phosphorylation of PTP α on Tyr⁷⁸⁹, which then decreased in a time-dependent manner after IL-1 treatment (Fig. 6D).

Functional Interactions between PTP α and IP₃R—Because the tyrosine phosphorylation state of the IP₃R dictates its Ca²⁺ conductance (64–66), we examined the effects of IL-1 and PTP α on the phosphorylation state of IP₃R1, which is the most prominent isoform in fibroblasts (58). For this assay IP₃R1 was immunoprecipitated from whole cell lysates of PTP $\alpha^{+/+}$ and PTP $\alpha^{-/-}$ murine fibroblasts, as well as genetically modified NIH3T3^{PTP α} cells or cells with the catalytically inert PTP α mutant (NIH3T3^{CCSS}) that had been treated with IL-1 or vehicle control and blotted with a phosphotyrosine antibody. In response to IL-1, phosphorylation of IP₃R1 in PTP $\alpha^{+/+}$ was sharply increased (maximal at 2 min) and declined thereafter (Fig. 7A). Further, the phosphorylation of IP₃R1 was dependent on the presence of catalytically active PTP α , because cells lacking PTP α or expressing the catalytically inactive (CCSS) PTP α showed no detectable IL-1-induced phosphorylation of IP₃R1 (Fig. 7B).

We next considered whether IP₃R1 immunopurified from wild-type PTP α cells could be directly dephosphorylated by PTP α . Purified IP₃R1 bound to protein A-Sepharose beads was exposed to active Fyn in a kinase buffer to promote its tyrosine phosphorylation. Next, the phosphorylated IP₃R1 protein was incubated with the recombinant cytosolic domain of PTP α . Active Fyn was able to phosphorylate IP₃R1, but the recombinant cytoplasmic domain of PTP α was unable to dephosphorylate IP₃R1 (Fig. 7C). As a control, recombinant cPTP α readily dephosphorylated recombinant SHP-2 (data not shown). Consequently, IP₃R1 is not a direct substrate of PTP α . Instead, we considered that the ability of PTP α to activate SFK (c-Src or Fyn) may be achieved by dephosphorylating the carboxyl-terminal inhibitory tyrosine residue (Tyr(P)⁵²⁹ of Src), thereby enhancing the catalytic activity of these kinases

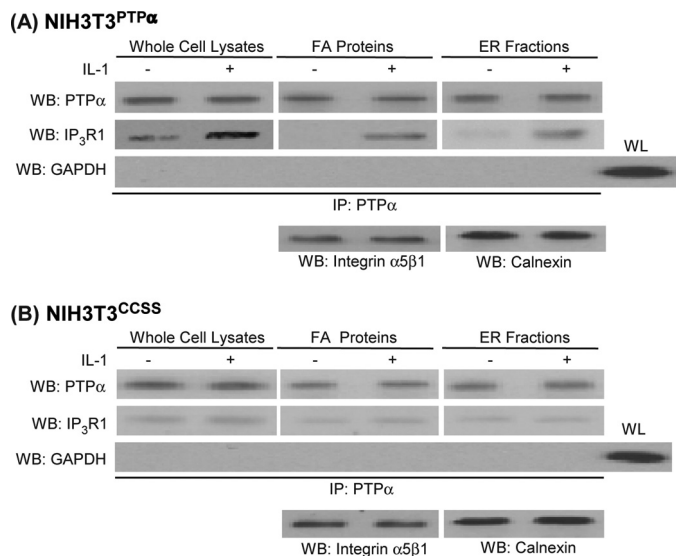


FIGURE 4. **PTP α associates with IP₃R1.** PTP α was immunoprecipitated (IP) from whole cell lysates, FA proteins, or ER fractions prepared from vehicle (–) or IL-1 (+) treated cells. A, NIH3T3^{PTP α} cells; B, NIH3T3^{CCSS} cells. Immunoprecipitates were immunoblotted for PTP α , IP₃R1, or GAPDH. For loading controls, focal adhesion proteins were immunoblotted for α 5 β 1 integrin, and for the ER fraction immunoblotting for calnexin was used. WB, Western blotting.

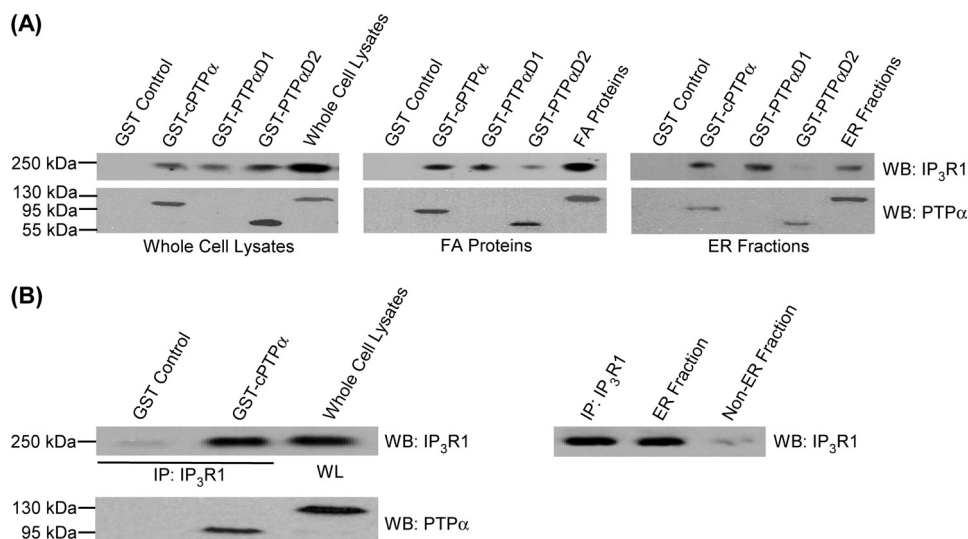


FIGURE 5. **PTP α associates with IP₃R1.** GST pull-down experiments to show association between PTP α and IP₃R1 *in vitro* are shown. A, glutathione-agarose (GST) beads bound to bacterially expressed cPTP α , cPTP α D1, or cPTP α D2 fusion proteins or GST control beads were incubated with whole cell lysates (WL), FA proteins, and ER fractions from PTP α^{Rescue} cells. The materials bound to the beads were analyzed by immunoblotting for IP₃R1. Whole cell lysates, FA proteins, and ER fractions were also immunoblotted for IP₃R1. Note that the protein products of the domain deleted constructs (cPTP α D1 or cPTP α D2) have lower molecular masses (~60 kDa) compared with the cytosolic cPTP α (95 kDa) or full-length PTP α (130 kDa). B, GST-cPTP α or GST control fusion proteins were incubated with IP₃R1 that was IP purified from whole cell lysates of PTP α^{Rescue} cells. WB, Western blotting.

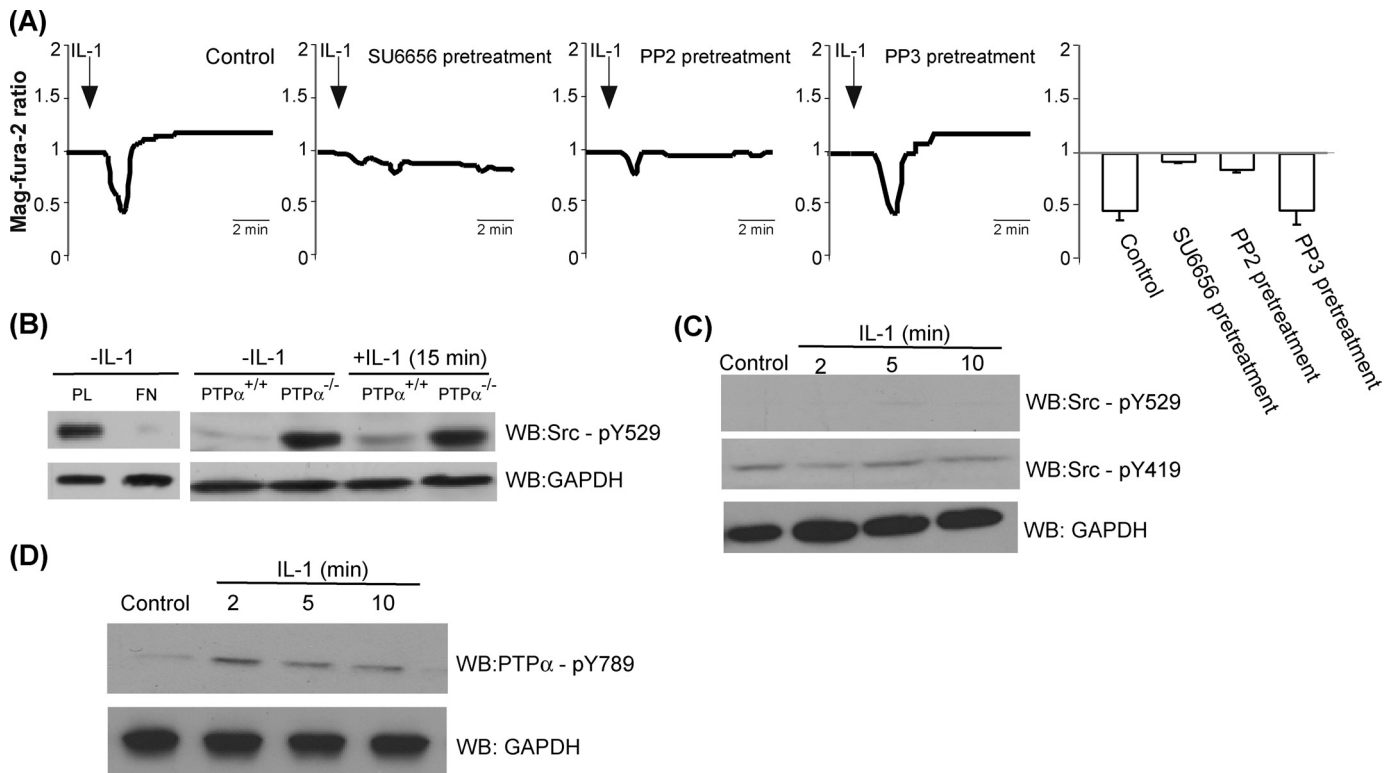


FIGURE 6. Involvement of Src kinase and PTP α in IL-1-induced ER Ca²⁺ release. *A*, ER-Ca²⁺ release by IL stimulation was inhibited by Src kinase inhibitors SU6656 and PP-2, but not by the inactive analog PP3. PTP α ^{+/+} cells were pretreated with vehicle control, SU6656 (5 μ M for 1 h), PP2 (10 μ M for 30 min), or PP3 (10 μ M for 30 min) and stimulated with IL-1 prior to mag-fura-2-loading. The data in histograms are the means \pm S.E. of mag-fura-2 ratios. *B*, *left panel*, Src activation requires integrin stimulation. Whole cell lysates of PTP α ^{+/+} cells plated on PL or FN were immunoblotted for antibodies to phospho-Src (pY529) or GAPDH. *Right panel*, indicated cell types were treated with vehicle or IL-1 for 15 min and immunoblotted for phospho-Src (pY529). *C*, Src (pY529) levels remain low from 0–10 min after IL-1 treatment, whereas Src (pY419) remain constant. Whole cell lysates of PTP α ^{+/+} cells were stimulated with IL-1 (20 ng/ml for 2, 15, or 10 min) or vehicle control and were immunoblotted for antibodies to phospho-Src (Tyr⁵²⁹) or phospho-Src (Tyr⁴¹⁹) or GAPDH. *D*, levels of PTP α (Tyr⁷⁸⁹) after IL-1 treatment. PTP α ^{+/+} cells were treated with or without IL-1 (20 ng/ml) for indicated time periods, and whole cell lysates were immunoblotted with antibodies to PTP α (Tyr⁷⁸⁹) and GAPDH. *WB*, Western blotting.

(30, 31, 61). We examined this possibility by first pretreating wild-type PTP α cells with the SFK inhibitor, SU6656. This treatment blocked IL-1-induced phosphorylation of IP₃R1 (Fig. 7D), indicating that the catalytic activity of SFK is required for IL-1-induced phosphorylation of the IP₃R1. We confirmed the ability of SU6656 to reduce the catalytic activity of Src by examining the Tyr⁵²⁹ inhibitory residue of Src. For this experiment, PTP α wild-type cells were treated with SU6656 for 1 h and stimulated with or without IL-1 for 30 min. When the whole cell lysates were immunoblotted for Tyr(P)⁵²⁹, increased levels of Tyr(P)⁵²⁹ were observed after SU6656 treatment (Fig. 7E).

We examined whether SFKs associate with IP₃R1 in response to IL-1. Wild-type PTP α cells were treated with IL-1. IP₃R1 was immunoprecipitated from cell lysates and immunoblotted with SFKs or c-Src specific antibodies. Time course experiments showed that SFKs associated with IP₃R1 after IL-1 and that in particular, c-Src was specifically detected in association with IP₃R1 (Fig. 7F). However, this association was dependent on the presence of PTP α , because in PTP α -null cells, the IL-1-induced association of Src with IP₃R1 was abolished (Fig. 7F, *middle panel*). In a similar experimental design, we prepared PTP α immunoprecipitates and immunoblotted for Src and c-Src (Fig. 7G). These data showed that PTP α associates with SFK (and specifically c-Src) in response to IL-1 in a time-dependent manner. Taken together with the earlier data showing that catalytically active PTP α associates with IP₃R1 in focal adhesions and ER preparations in response to IL-1 treatment (Fig. 4), we conclude that PTP α may mediate IL-1-induced Ca²⁺ signaling by acting as an adaptor to link IP₃R1 to c-Src.

ically active PTP α associates with IP₃R1 in focal adhesions and ER preparations in response to IL-1 treatment (Fig. 4), we conclude that PTP α may mediate IL-1-induced Ca²⁺ signaling by acting as an adaptor to link IP₃R1 to c-Src.

DISCUSSION

Our major finding is that PTP α provides an important structural linkage between focal adhesions and the ER, in part through its interactions with IP₃R1 and c-Src. In previous work (46, 58) we found rapid, focal adhesion-dependent release of Ca²⁺ from the ER in response to IL-1, suggesting a functional relationship between these different organelles, as well as spatial sequestration of signaling molecules involved in Ca²⁺ signaling (14). In view of these findings, we have sought to define the proteins that mediate this spatial selectivity and that enable focal adhesion restriction of IL-1 signaling.

Src—We found that inhibition of Src kinase activity with SU6656 or PP2 effectively blocked IL-1-induced IP₃R1 phosphorylation and ER Ca²⁺ release, indicating the importance of SFKs in focal adhesion-dependent calcium signaling initiated by IL-1. SFKs are pivotal for integrin-mediated signaling during cell adhesion and spreading because of their kinase-dependent and kinase-independent activities (67). Among the SFKs, c-Src and Fyn are dephosphorylated by PTP α on their inhibitory carboxyl-terminal tyrosine residue, which enhances their kinase

PTP α and Focal Adhesions

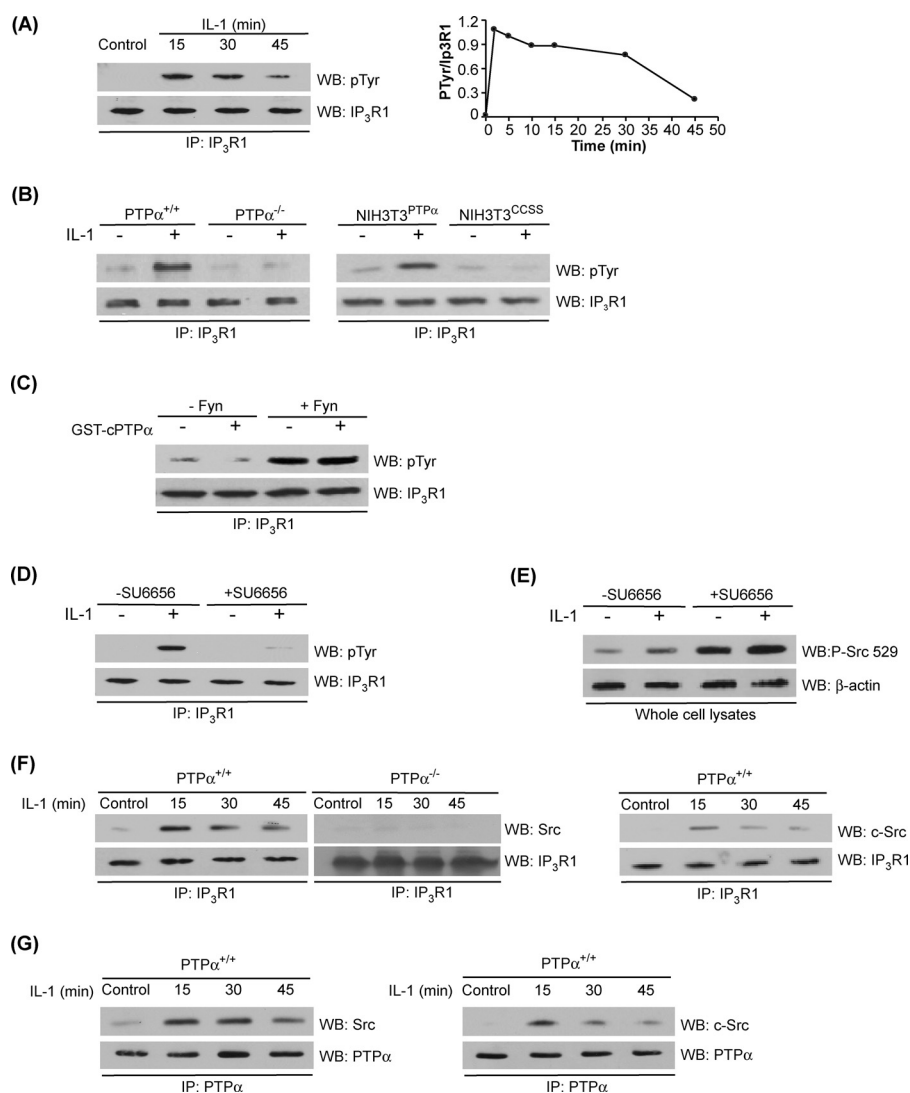


FIGURE 7. Tyrosine phosphorylation of IP₃R1: regulation by PTP α and Src. *A*, tyrosine phosphorylation of IP₃R1 rapidly increases after IL-1 treatment and then declines subsequently. IP₃R1 was immunopurified (IP) from whole cell lysates of PTP $\alpha^{+/+}$ cells that had been stimulated with or without IL-1, and immunoblotted for phosphotyrosine (pTyr, upper panel). The lower panel shows protein levels of immunoprecipitated IP₃R1. The line graph on the right shows the ratios of the blot densities of tyrosine-phosphorylated IP₃R1 to IP₃R1 over the full time course. *B*, tyrosine phosphorylation of IP₃R1 after IL-1 stimulation requires catalytically active PTP α . IP₃R1 was immunopurified from whole cell lysates of PTP $\alpha^{+/+}$, PTP $\alpha^{-/-}$, NIH3T3^{PTP α} , and NIH3T3^{CCSS} cells that had been stimulated with (+) or without (-) IL-1. Immunoprecipitates were immunoblotted for phosphotyrosine (pTyr, upper panel) or IP₃R1 (lower panel). *C*, IP₃R1 phosphorylation is not affected by PTP α . *In vitro* phosphorylation was analyzed by incubating immunopurified IP₃R1 from wild-type PTP α cells in presence or absence of active Fyn and then incubated with GST-cPTP α fusion protein. Phosphorylation was analyzed by immunoblotting with anti-phosphotyrosine antibody (pTyr, upper panel). The lower panel shows protein levels of immunopurified IP₃R1. *D*, tyrosine phosphorylation of IP₃R1 is dependent on catalytically active SFK. IP₃R1 was immunoprecipitated from PTP $\alpha^{+/+}$ cells that had been pretreated with SU6656 (5 μ M for 1 h) or vehicle and then treated with (+) or without (-) IL-1. Immunoprecipitates were immunoblotted for phosphotyrosine (pTyr, upper panel) or IP₃R1 (lower panel). *E*, cells treated with Src inhibitor exhibit high levels of Src (Tyr(P)⁵²⁹). The cells were preincubated with SU6656 (5 μ M for 1 h) and then treated with IL-1 (+) or vehicle (-) for 10 min. The cell lysates were immunoblotted for phosphorylation of the carboxyl-terminal inhibitory tyrosine residue of Src (Tyr(P)⁵²⁹). *F*, IL-1 promotes association of IP₃R1 with SFK and c-Src and PTP α is required for interactions between Src and IP₃R1. Left panel, PTP $\alpha^{+/+}$ cells were stimulated with IL-1 as indicated. Middle panel, PTP $\alpha^{-/-}$ cells were stimulated with IL-1 as indicated. IP₃R1 immunoprecipitates were immunoblotted for either SFK (left and middle panels, Src) or c-Src (right panel). *G*, IL-1 promotes association of PTP α with SFK and c-Src. PTP $\alpha^{+/+}$ cells were stimulated with IL-1. PTP α immunoprecipitates were immunoblotted for either SFK (left panel, Src) or c-Src (right panel). After longer exposure to IL-1, the association dissipated. WB, Western blotting.

activity (31, 54). Consistent with these reports we found that PTP α was essential for enabling signaling downstream of SFKs because PTP α -null cells exhibited very high levels of phospho-

rylation of the inhibitory Tyr⁵²⁹ residue and showed no IL-1-induced Ca²⁺ signaling. When the inhibitory carboxyl-terminal tyrosine residue was dephosphorylated in cells that have intact focal adhesions and express catalytically active PTP α , SFK catalytic activity enabled direct phosphorylation of IP₃R1 and, subsequently, Ca²⁺ release from the ER. Further, our immunoprecipitation studies showed that c-Src was one of the SFKs that associated with IP₃R1, contemporaneous with enhanced ER Ca²⁺ release. Thus c-Src could be one of the SFKs that directly phosphorylate and activate IP₃R1, although other SFKs such as Fyn and Lyn could also be involved in this process (59, 60).

Importantly, the activation of SFK is only achieved in the presence of intact FA and PTP α and is required for the immediate Ca²⁺ response in cells treated with IL-1. Eventually continued IL-1 treatment longer than 15 min led to the inactivation of Src and this correlated temporally with increased phosphorylation of inhibitory residue (Tyr⁵²⁹) of Src and diminished phosphorylation of PTP α at Tyr⁷⁸⁹, consistent with the notion that Tyr(P)⁷⁸⁹ of PTP α is important for regulating Src activation (24, 54).

IP₃ Receptors—IP₃Rs are Ca²⁺-permeable channels located on the membranes of organelles with releasable Ca²⁺ stores (48). Cell surface biotinylation studies have shown that ~5–14% of total IP₃ receptors are localized to the plasma membranes of several cell types (49). We have previously found abundant IP₃R1 isoform in the ER of human gingival fibroblasts (58) and in the ER of murine fibroblasts used here. Notably, IP₃R1 was also enriched in focal adhesion-associated proteins, suggesting that IP₃R1 may link the ER to FAs at specific cellular sites. As a result of the critical importance of IP₃ receptors in Ca²⁺ release from the ER (51) and their central role demonstrated here

in IL-1-induced Ca²⁺ signaling, we focused our studies on IP₃R as a Ca²⁺ release channel and as a candidate protein for linking the ER to FAs.

The precise function of IP₃R is mediated by the coordinated actions of Ca²⁺, phosphorylation, and nucleotides. Ca²⁺ exerts biphasic control over IP₃R (68–70): stimulation by positive feedback at physiological concentrations and inhibition at low micromolar [Ca²⁺] (71, 72). Phosphorylation of IP₃R1 increases its sensitivity to Ca²⁺ conductance at even low IP₃ levels (73). We found that IP₃R1 was strongly tyrosine-phosphorylated in response to IL-1, particularly at early time periods (prior to 15 min); this phosphorylation diminished rapidly thereafter. Because our immunoprecipitation studies showed temporal correlations between increased IP₃R1 phosphorylation and IP₃R1 association with SFK and c-Src, it seems likely that SFKs promote Ca²⁺ signaling not only by phosphorylating and activating phospholipases that generate IP₃ but also by directly phosphorylating IP₃R (Tyr³⁵³) and augmenting Ca²⁺ channel activity (59, 73). Further, tyrosine phosphorylation renders the IP₃R insensitive to rising inhibitory Ca²⁺ levels (59), which would otherwise inhibit its open probability.

In addition to its role as a Ca²⁺ channel in the ER membrane, IP₃R has been implicated in many adaptor functions because of its association with various phosphatases (51). Further, the association of IP₃R with the FA proteins vinculin, α -actinin, and talin (52) suggest that IP₃R could interact with other critical focal adhesion signaling molecules. We found here that IL-1 up-regulated the relative abundance of IP₃R1 in ER fractions as well as in FA-associated proteins, but this enrichment only occurred in cells expressing catalytically active PTP α . By total internal reflection fluorescence microscopy imaging of subplasma membrane compartments, we observed that PTP α colocalizes with IP₃R1. Consistent with these observations, immunoprecipitation and pulldown assays with purified proteins indicated that PTP α associated with IP₃R1. However, we found that IP₃R1 was not a substrate of PTP α . Instead, SFKs and, in particular, c-Src associated with and likely phosphorylated IP₃R in response to IL-1. Notably, the disruption of the enzymatic activity of PTP α impaired the ability of IP₃R1 to associate with PTP α and Src. Apparently, the adaptor function of PTP α relies on the integrity of its catalytic domain because only point mutations in the D1 (C433S) and D2 (C723S) domains were required to disrupt IL-1-induced tyrosine phosphorylation of IP₃R1, Ca²⁺ signaling, and association of IP₃R1 with PTP α . Notably, the association of IP₃R1 with PTP α in response to IL-1 may mediate physical approximation of FAs with the ER. By this mechanism PTP α may indirectly control IL-1-induced tyrosine phosphorylation and enhancement of IP₃R1 Ca²⁺ channel activity, possibly via the activation of c-Src or Fyn.

We conclude that PTP α plays two essential roles in IL-1-induced Ca²⁺ signaling. First, PTP α dephosphorylates and activates SFKs, in response to integrin stimulation, that are essential for enabling Ca²⁺ release through IP₃ receptors in the ER. Second, PTP α provides a critical structural link between FAs and the ER as a result of its interactions with IP₃R1 and c-Src. This trimolecular interaction is needed for IL-1-induced Ca²⁺ release.

REFERENCES

- O'Neill, L. A., and Dinarello, C. A. (2000) *Immunol. Today* **21**, 206–209
- Dunne, A., and O'Neill, L. A. (2003) *Sci. STKE* **2003**, re3
- Gasse, P., Mary, C., Guenon, I., Noulin, N., Charron, S., Schnyder-Candrian, S., Schnyder, B., Akira, S., Quesniaux, V. F., Lagente, V., Ryffel, B., and Couillin, I. (2007) *J. Clin. Invest.* **117**, 3786–3799
- Dayer, J. M. (2003) *Rheumatology* **42**, (Suppl. 2) ii3–10
- Boyle, D. L., Han, Z., Rutter, J. L., Brinckerhoff, C. E., and Firestein, G. S. (1997) *Arthritis Rheum.* **40**, 1772–1779
- Graves, D. T., and Cochran, D. (2003) *J. Periodontol.* **74**, 391–401
- Fagarasan, M. O., Aiello, F., Muegge, K., Durum, S., and Axelrod, J. (1990) *Proc. Natl. Acad. Sci. U.S.A.* **87**, 7871–7874
- Hamid, Q. A., Reddy, P. J., Tewari, M., Uematsu, S., Tuncay, O. C., and Tewari, D. S. (2000) *Cytokine* **12**, 1609–1619
- Kumkumian, G. K., Lafyatis, R., Remmers, E. F., Case, J. P., Kim, S. J., and Wilder, R. L. (1989) *J. Immunol.* **143**, 833–837
- Caron, J. P., Tardif, G., Martel-Pelletier, J., DiBattista, J. A., Geng, C., and Pelletier, J. P. (1996) *Am. J. Vet. Res.* **57**, 1631–1634
- Reunanen, N., Westermarck, J., Hakkinen, L., Holmstrom, T. H., Elo, L., Eriksson, J. E., and Kahari, V. M. (1998) *J. Biol. Chem.* **273**, 5137–5145
- Lo, Y. Y., Luo, L., McCulloch, C. A., and Cruz, T. F. (1998) *J. Biol. Chem.* **273**, 7059–7065
- Wang, Q., Downey, G. P., Choi, C., Kapus, A., and McCulloch, C. A. (2003) *FASEB J.* **17**, 1898–1900
- Luo, L., Cruz, T., and McCulloch, C. (1997) *Biochem. J.* **324**, 653–658
- Aplin, A. E., and Juliano, R. L. (1999) *J. Cell Sci.* **112**, 695–706
- Garrington, T. P., and Johnson, G. L. (1999) *Curr. Opin. Cell Biol.* **11**, 211–218
- Burridge, K., and Chrzanowska-Wodnicka, M. (1996) *Annu. Rev. Cell Dev. Biol.* **12**, 463–518
- Zaidel-Bar, R., Cohen, M., Addadi, L., and Geiger, B. (2004) *Biochem. Soc. Trans.* **32**, 416–420
- Kirchner, J., Kam, Z., Tzur, G., Bershadsky, A. D., and Geiger, B. (2003) *J. Cell Sci.* **116**, 975–986
- Ilic, D., Furuta, Y., Kanazawa, S., Takeda, N., Sobue, K., Nakatsuji, N., Nomura, S., Fujimoto, J., Okada, M., and Yamamoto, T. (1995) *Nature* **377**, 539–544
- Klinghoffer, R. A., Sachsenmaier, C., Cooper, J. A., and Soriano, P. (1999) *EMBO J.* **18**, 2459–2471
- Harder, K. W., Moller, N. P., Peacock, J. W., and Jirik, F. R. (1998) *J. Biol. Chem.* **273**, 31890–31900
- Lammers, R., Lerch, M. M., and Ullrich, A. (2000) *J. Biol. Chem.* **275**, 3391–3396
- Chen, M., Chen, S. C., and Pallen, C. J. (2006) *J. Biol. Chem.* **281**, 11972–11980
- Schlessinger, J. (2000) *Cell* **100**, 293–296
- Wang, Q., Downey, G. P., Herrera-Abreu, M. T., Kapus, A., and McCulloch, C. A. (2005) *J. Biol. Chem.* **280**, 8397–8406
- Ostman, A., and Bohmer, F. D. (2001) *Trends Cell Biol.* **11**, 258–266
- Schlessinger, J. (2000) *Cell* **103**, 211–225
- Carragher, N. O., and Frame, M. C. (2004) *Trends Cell Biol.* **14**, 241–249
- Zheng, X. M., Wang, Y., and Pallen, C. J. (1992) *Nature* **359**, 336–339
- den Hertog, J., Pals, C. E., Peppelenbosch, M. P., Tertoolen, L. G., de Laat, S. W., and Kruijer, W. (1993) *EMBO J.* **12**, 3789–3798
- Stoker, A. W. (2005) *J. Endocrinol.* **185**, 19–33
- Li, L., and Dixon, J. E. (2000) *Semin. Immunol.* **12**, 75–84
- Serra-Pages, C., Kedersha, N. L., Fazikas, L., Medley, Q., Debant, A., and Streuli, M. (1995) *EMBO J.* **14**, 2827–2838
- Weng, L. P., Wang, X., and Yu, Q. (1999) *Genes Cells* **4**, 185–196
- Sap, J., D'Eustachio, P., Givol, D., and Schlessinger, J. (1990) *Proc. Natl. Acad. Sci. U.S.A.* **87**, 6112–6116
- Lim, K. L., Lai, D. S., Kalousek, M. B., Wang, Y., and Pallen, C. J. (1997) *Eur. J. Biochem.* **245**, 693–700
- Wang, Y., and Pallen, C. J. (1991) *EMBO J.* **10**, 3231–3237
- Parsons, J. T. (2003) *J. Cell Sci.* **116**, 1409–1416
- Ponniah, S., Wang, D. Z., Lim, K. L., and Pallen, C. J. (1999) *Curr. Biol.* **9**, 535–538

41. Su, J., Muranjan, M., and Sap, J. (1999) *Curr. Biol.* **9**, 505–511
42. Vacaresse, N., Moller, B., Danielsen, E. M., Okada, M., and Sap, J. (2008) *J. Biol. Chem.* **283**, 35815–35824
43. Zeng, L., Si, X., Yu, W. P., Le, H. T., Ng, K. P., Teng, R. M., Ryan, K., Wang, D. Z., Ponniah, S., and Pallen, C. J. (2003) *J. Cell Biol.* **160**, 137–146
44. Herrera Abreu, M. T., Penton, P. C., Kwok, V., Vachon, E., Shalloway, D., Vidali, L., Lee, W., McCulloch, C. A., and Downey, G. P. (2008) *Am. J. Physiol. Cell Physiol.* **294**, C931–C944
45. von Wichert, G., Jiang, G., Kostic, A., De Vos, K., Sap, J., and Sheetz, M. P. (2003) *J. Cell Biol.* **161**, 143–153
46. Wang, Q., Downey, G. P., Bajenova, E., Abreu, M., Kapus, A., and McCulloch, C. A. (2005) *FASEB J.* **19**, 837–839
47. Berridge, M. J., Lipp, P., and Bootman, M. D. (2000) *Nat. Rev.* **1**, 11–21
48. Khan, A. A., Steiner, J. P., Klein, M. G., Schneider, M. F., and Snyder, S. H. (1992) *Science* **257**, 815–818
49. Tanimura, A., Tojyo, Y., and Turner, R. J. (2000) *J. Biol. Chem.* **275**, 27488–27493
50. Khan, A. A., Steiner, J. P., and Snyder, S. H. (1992) *Proc. Natl. Acad. Sci. U.S.A.* **89**, 2849–2853
51. Patterson, R. L., Boehning, D., and Snyder, S. H. (2004) *Annu. Rev. Biochem.* **73**, 437–465
52. Sugiyama, T., Matsuda, Y., and Mikoshiba, K. (2000) *FEBS Lett.* **466**, 29–34
53. McCulloch, C. A., Downey, G. P., and El-Gabalawy, H. (2006) *Nat. Rev.* **5**, 864–876
54. Zheng, X. M., Resnick, R. J., and Shalloway, D. (2000) *EMBO J.* **19**, 964–978
55. Plopper, G., and Ingber, D. E. (1993) *Biochem. Biophys. Res. Commun.* **193**, 571–578
56. Oakes, S. A., Scorrano, L., Opferman, J. T., Bassik, M. C., Nishino, M., Pozzan, T., and Korsmeyer, S. J. (2005) *Proc. Natl. Acad. Sci. U.S.A.* **102**, 105–110
57. Arora, P. D., Ma, J., Min, W., Cruz, T., and McCulloch, C. A. (1995) *J. Biol. Chem.* **270**, 6042–6049
58. Wang, Q., Herrera Abreu, M. T., Siminovitch, K., Downey, G. P., and McCulloch, C. A. (2006) *J. Biol. Chem.* **281**, 31093–31105
59. Jayaraman, T., Ondrias, K., Ondriasova, E., and Marks, A. R. (1996) *Science* **272**, 1492–1494
60. Yokoyama, K., Su Ih, I. H., Tezuka, T., Yasuda, T., Mikoshiba, K., Tarakhovsky, A., and Yamamoto, T. (2002) *EMBO J.* **21**, 83–92
61. Bhandari, V., Lim, K. L., and Pallen, C. J. (1998) *J. Biol. Chem.* **273**, 8691–8698
62. Roskoski, R., Jr. (2005) *Biochem. Biophys. Res. Commun.* **331**, 1–14
63. Roskoski, R., Jr. (2004) *Biochem. Biophys. Res. Commun.* **324**, 1155–1164
64. Tang, T. S., Tu, H., Wang, Z., and Bezprozvanny, I. (2003) *J. Neurosci.* **23**, 403–415
65. Pieper, A. A., Brat, D. J., O'Hearn, E., Krug, D. K., Kaplin, A. I., Takahashi, K., Greenberg, J. H., Ginty, D., Molliver, M. E., and Snyder, S. H. (2001) *Neuroscience* **102**, 433–444
66. Edwards, A., and Pallone, T. L. (2007) *Am. J. Physiol. Renal Physiol.* **293**, F1518–F1532
67. Kaplan, K. B., Swedlow, J. R., Morgan, D. O., and Varmus, H. E. (1995) *Genes Dev.* **9**, 1505–1517
68. Bezprozvanny, I., Watras, J., and Ehrlich, B. E. (1991) *Nature* **351**, 751–754
69. Finch, E. A., and Augustine, G. J. (1998) *Nature* **396**, 753–756
70. Miyakawa, T., Mizushima, A., Hirose, K., Yamazawa, T., Bezprozvanny, I., Kurosaki, T., and Iino, M. (2001) *EMBO J.* **20**, 1674–1680
71. Boehning, D., Joseph, S. K., Mak, D. O., and Foscett, J. K. (2001) *Biophys. J.* **81**, 117–124
72. Mak, D. O., McBride, S., and Foscett, J. K. (2001) *J. Gen. Physiol.* **117**, 435–446
73. Cui, J., Matkovich, S. J., deSouza, N., Li, S., Rosemblyt, N., and Marks, A. R. (2004) *J. Biol. Chem.* **279**, 16311–16316